Synthesis, crystal structure and EPR spectroscopic analysis of novel copper complexes formed from *N*-pyridyl-4-nitro-1,8-naphthalimide ligands

Jonathan A. Kitchen[a,b]*, Paulo N. Martinho,[c,d] Grace G. Morgan,[c] and Thorfinnur Gunnlaugsson[a]

Electronic Supporting Information (ESI)

X-ray crystallography

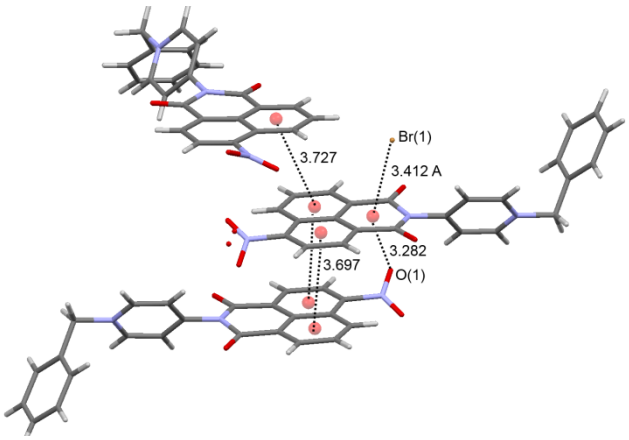

Figure S1: Perspective view of packing interactions in L_1Bn·Br showing π···π, NO_2···π and Br···π interactions.

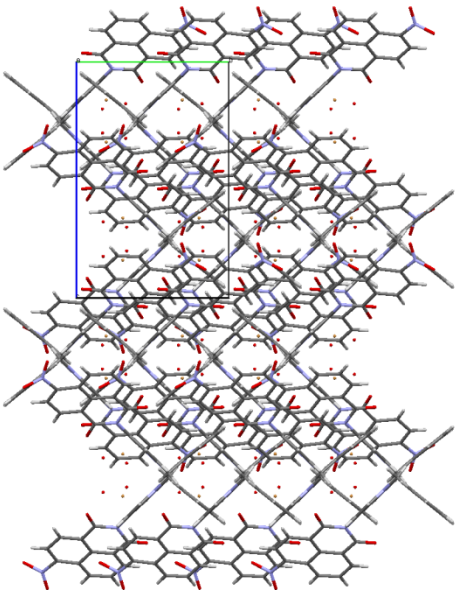

Figure S2: Perspective view of packing interactions in L1Bn·Br when viewed down the a-axis.

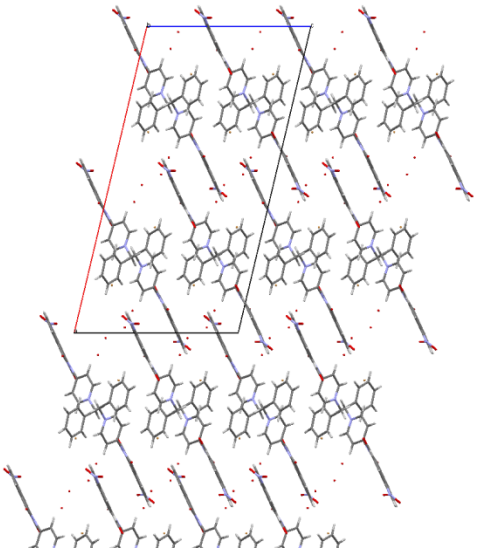

Figure S3: Perspective view of packing interactions in L1Bn·Br when viewed down the a-axis.

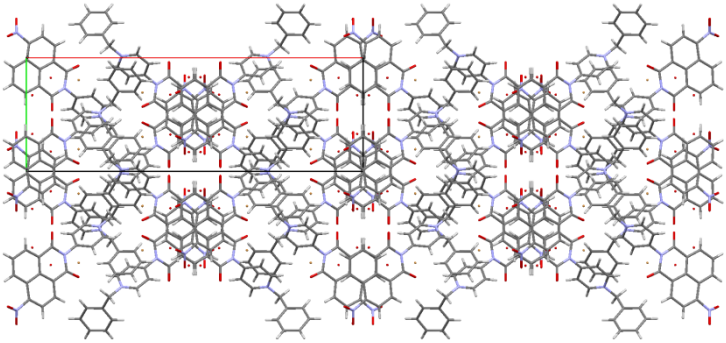

Figure S4: Perspective view of packing interactions in L1Bn·Br when viewed down the a-axis.

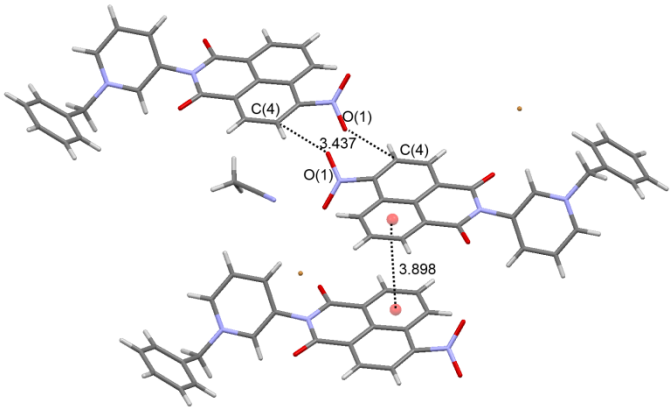

Figure S5: Perspective view of packing interactions in $L_2Bn \cdot Br$ showing $\pi\cdots\pi$ and C-H hydrogen bonding.

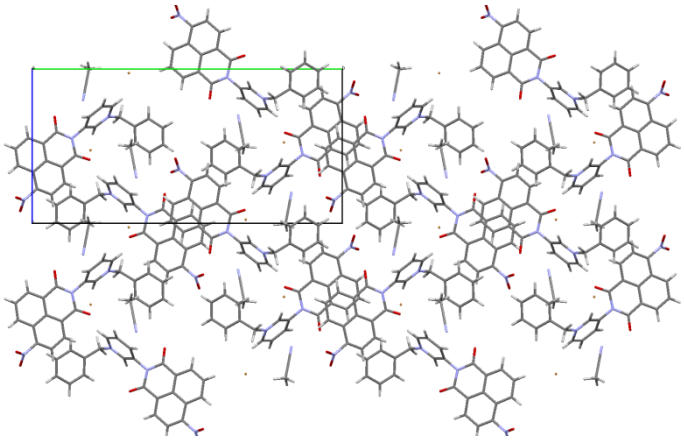

Figure S6: Perspective view of packing interactions in $L_2Bn \cdot Br$ when viewed down the a-axis.

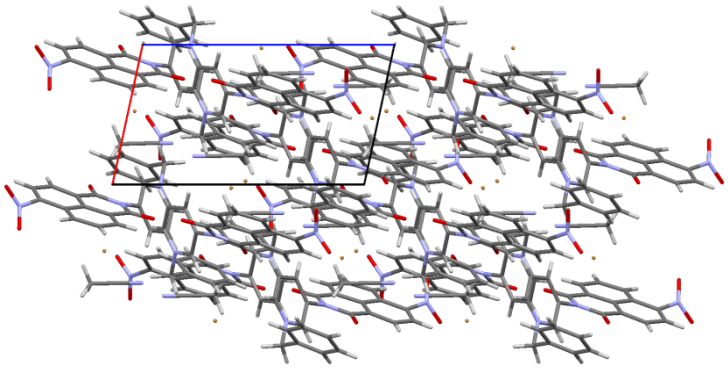

Figure S7: Perspective view of packing interactions in $L_2Bn \cdot Br$ when viewed down the b-axis.

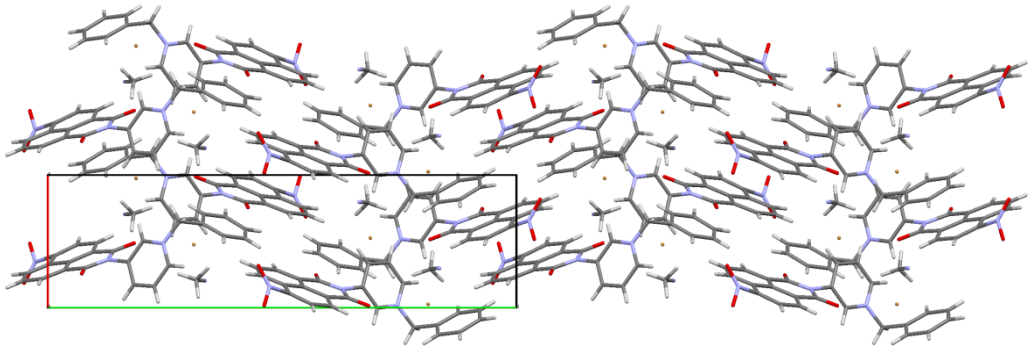

Figure S8: Perspective view of packing interactions in $L_2Bn \cdot Br$ when viewed down the c-axis.

Packing Interactions of Cu(II) complexes

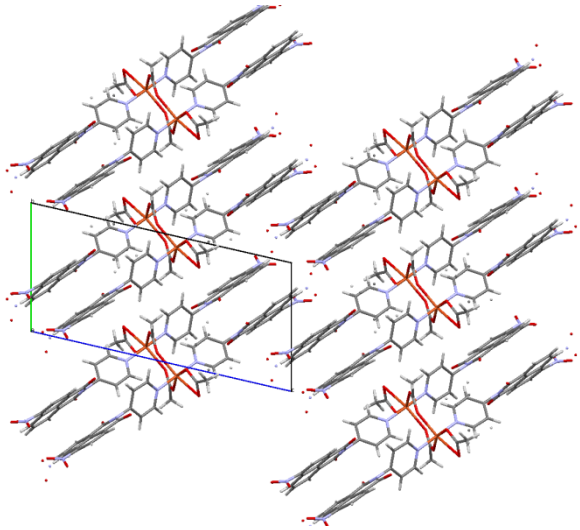

Figure S9: Perspective view of packing in 1 viewed down the a-axis.

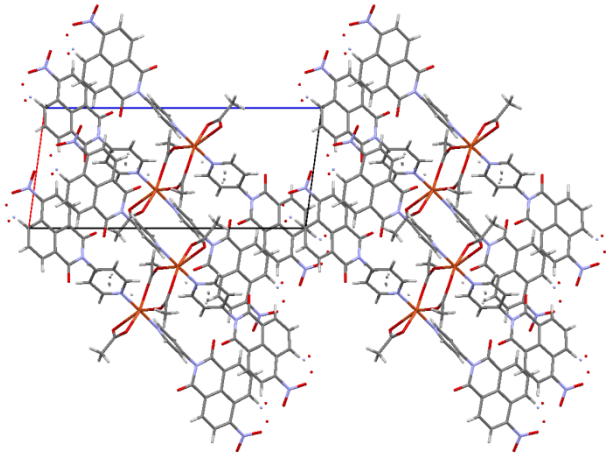

Figure S10: Perspective view of packing in 1 viewed down the b-axis.

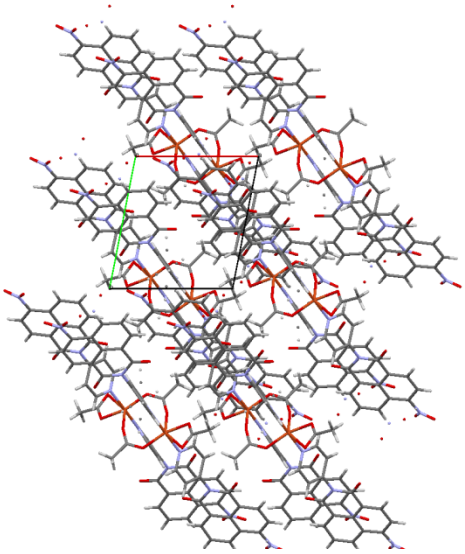

Figure S11: Perspective view of packing in 1 viewed down the c-axis.

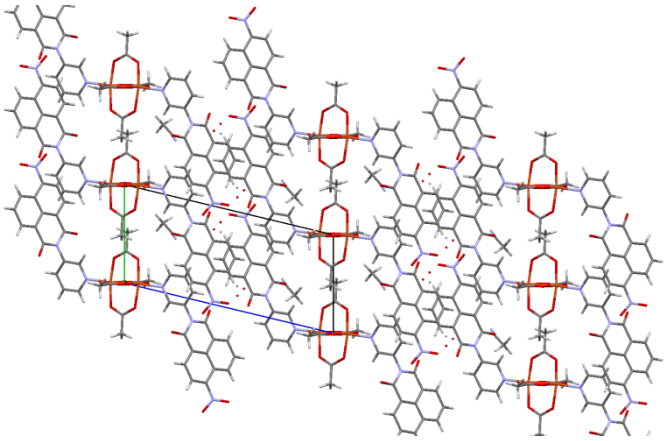

Figure S12: Perspective view of packing in 2 viewed down the a-axis.

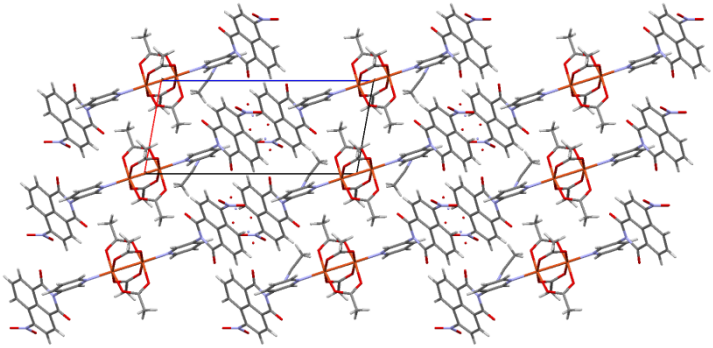

Figure S13: Perspective view of packing in 2 viewed down the b-axis.

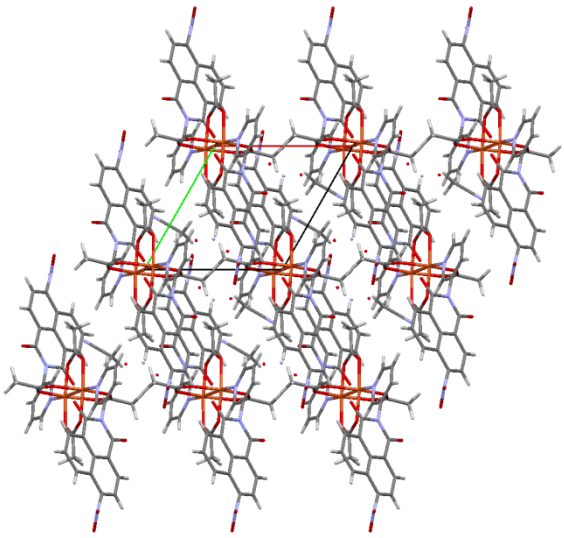

Figure S14: Perspective view of packing in 2 viewed down the c-axis.

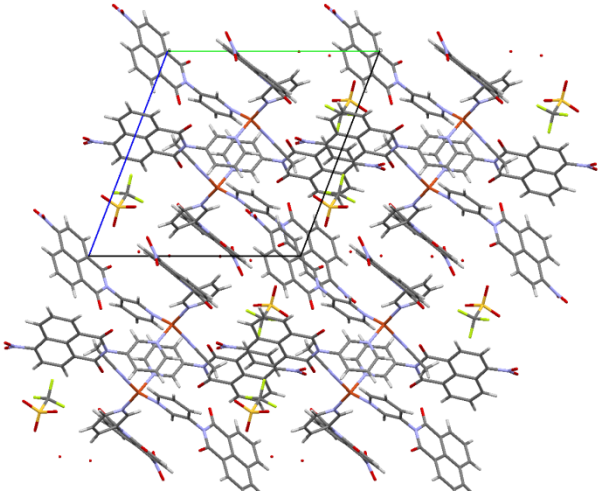

Figure S15: Perspective view of packing in 4 viewed down the a-axis.

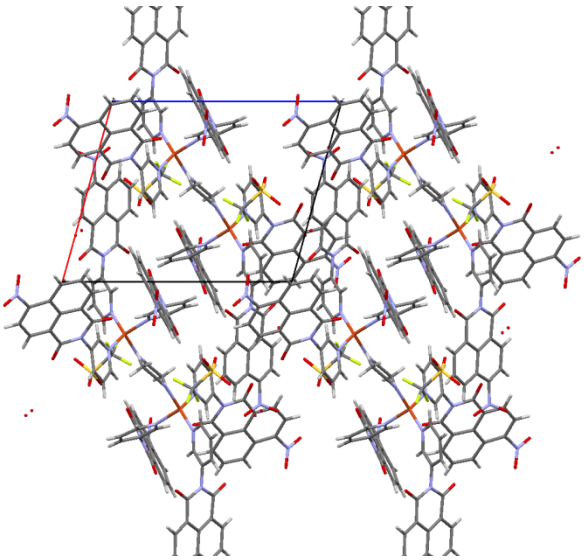

Figure S16: Perspective view of packing in 4 viewed down the b-axis.

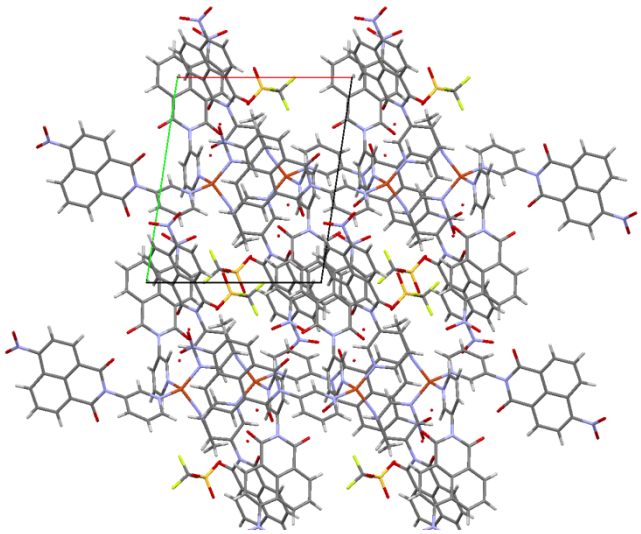

Figure S17: Perspective view of packing in 4 viewed down the c-axis.

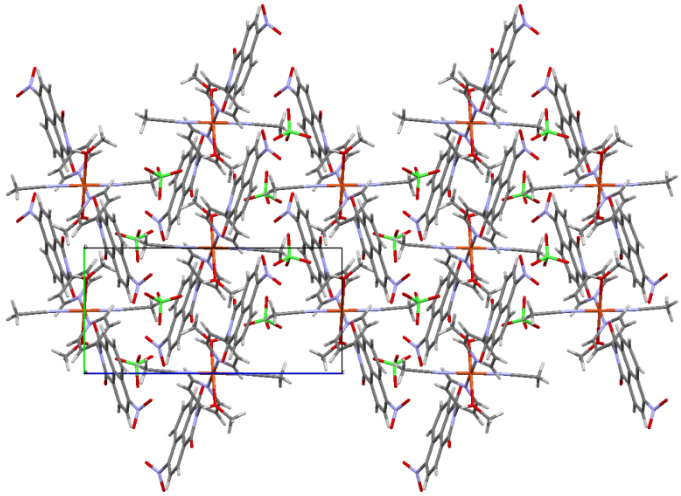

Figure S18: Perspective view of packing in 5 viewed down the a-axis

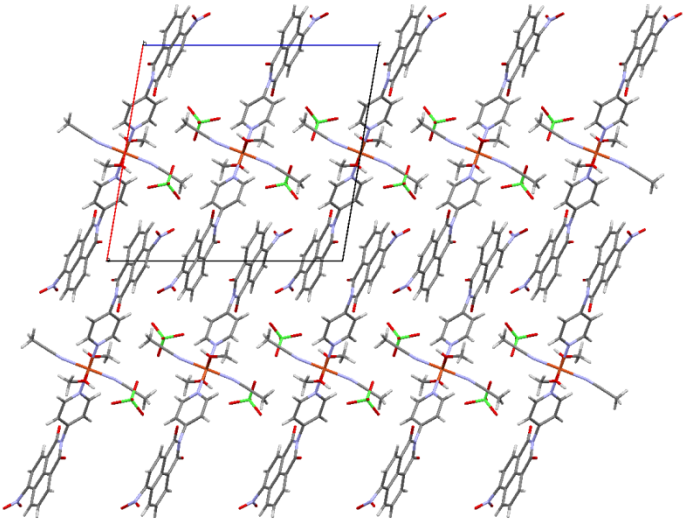

Figure S19: Perspective view of packing in 5 viewed down the b-axis

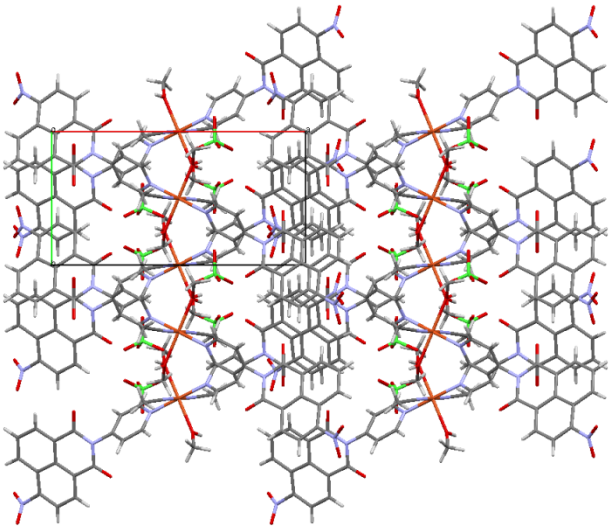

Figure S20: Perspective view of packing in 5 viewed down the c-axis

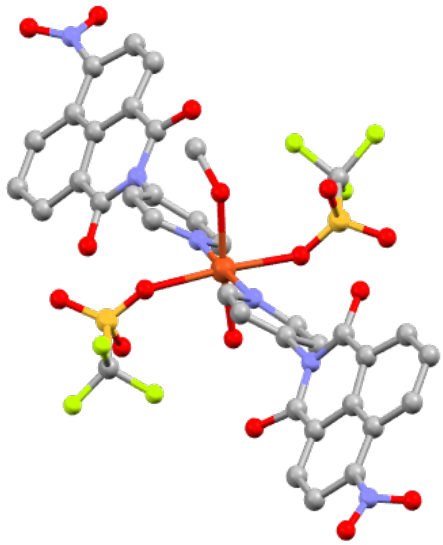

Figure S21: Connectivity of 3 as determined by X-ray crystal structure analysis on poor quality crystals.

EPR Spectroscopy

X-band electron paramagnetic resonance spectra of solid samples of compounds (**1**) – (**5**) were recorded at 293 and 113 K on a Magnettech Miniscope MS200 EPR spectrometer fitted with a MW frequency counter and a temperature controller. The measurements were performed with magnetic field centred at 323 mT and a field sweep of 600 mT. Modulation amplitude, microwave power and gain values are given below, the time constant in all measurements was 0 sec. g-values and hyperfine coupling constants are also listed.

(**1**) modulation amplitude = 0.7 mT; microwave power = 0.1585 mW; gain = 1. At T = 113 K $g_1 = 2.30$, $g_2 = 2.15$, $g_3 = 2.05$

(**2**) modulation amplitude = 0.7 mT; microwave power = 10 mW; gain = 50. At T = 113 K $g_1 = 17.9$, $g_3 = 1.13$ assigned together as $g_{\parallel}$; $g_2 = 1.13$ was assigned as $g_{\perp}$.

(**3**) modulation amplitude = 0.7 mT; microwave power = 0.1 mW; gain = 10. At T = 113 K $g_{\perp} = 2.05$, $g_{\parallel} = 2.32$, $A_{\parallel} = 19$ mT

(**5**) modulation amplitude = 0.7 mT; microwave power = 0.1585 mW; gain = 1. $g_{\perp} = 2.05$, $g_{\parallel} = 2.28$, $A_{\parallel} = 19$ mT.

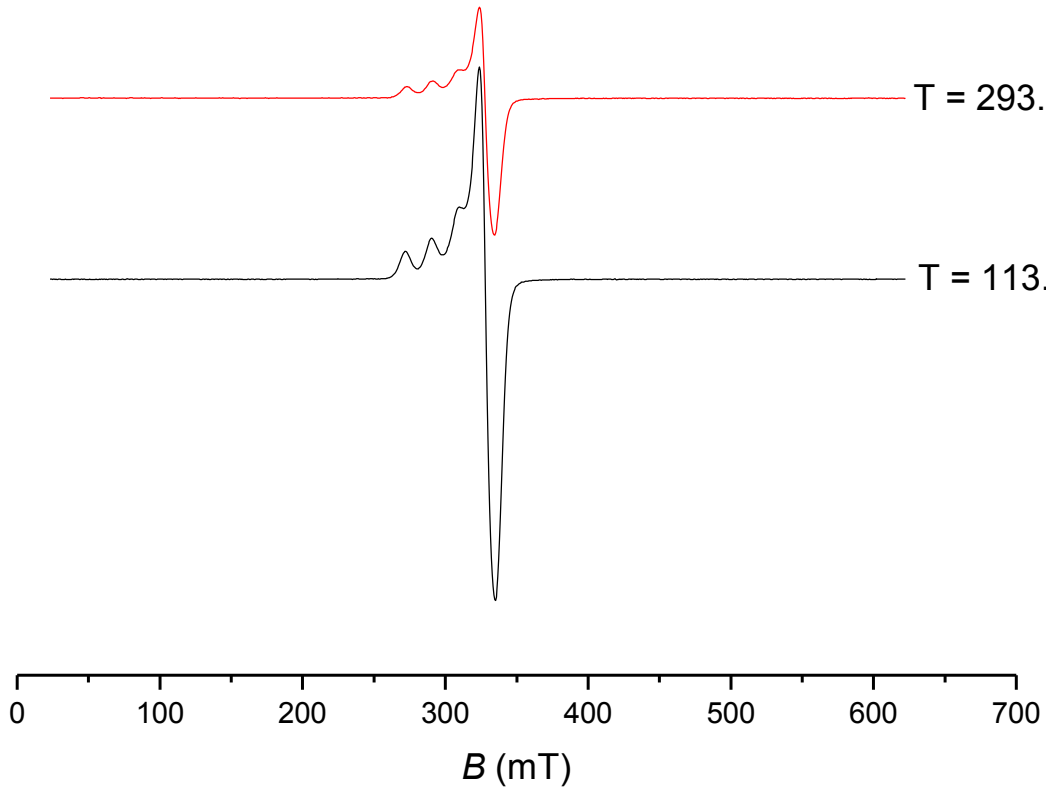

Figure S22. EPR spectra of (3) at 113 K and 293 K.

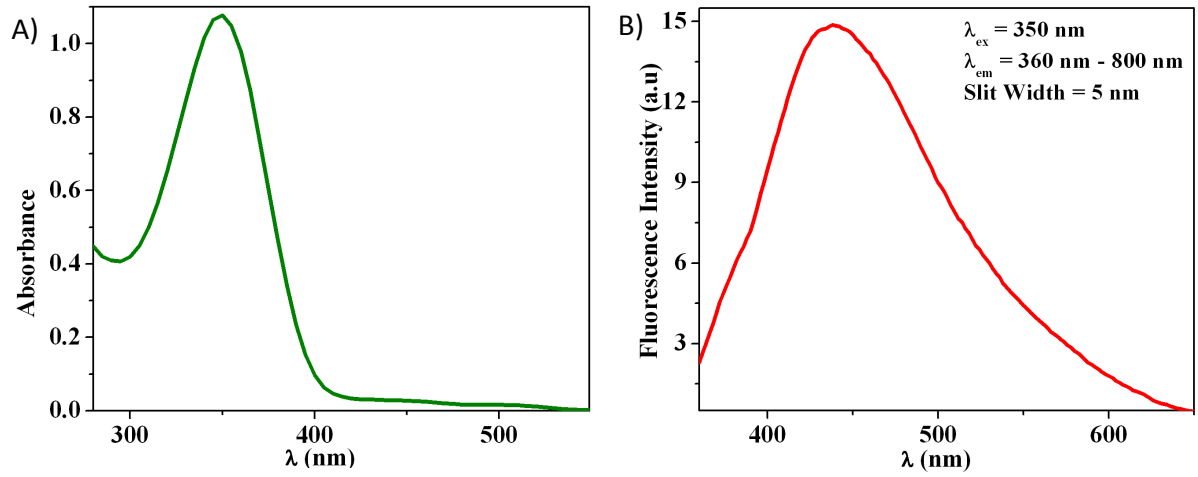

Figure S23. A) UV-vis absorption and B) fluorescence emission spectra of L1 in CH_3CN at RT.